buildings

MDPI

Article

Steady-State Thermal Properties of Rectangular Straw-Bales (RSB) for Building

Leonardo Conti *, Matteo Barbari and Massimo Monti

Department of Agricultural, Food and Forestry Systems (GESAAF)—Via San Bonaventura 13, 50145 Florence, Italy; matteo.barbari@unifi.it (M.B.); montistudio@centonuvole.com (M.M.)
* Correspondence: leonardo.conti@unifi.it; Tel.: +39-055-2755626

Academic Editor: Adrian Pitts
Received: 8 July 2016; Accepted: 11 October 2016; Published: 18 October 2016

Abstract: Straw is an inevitable product of cereal production and is available in huge quantities in the world. In order to use straw-bales as a building material, the characteristic values of the thermal performances should be determined. To not lose the benefits of the cheapness and sustainability of the material, the characteristics must be determined with simple and inexpensive means and procedures. This research aims to implement tools and methods focused at the determination of the thermal properties of straw-bales. For this study, the guidelines dictated by ASTM and ISO were followed. A measurement system consisting of a Metering Chamber (MC) was realized. The MC was placed inside a Climate Chamber (CC). During the test, a known quantity of energy is introduced inside MC. When the steady-state is reached, all the energy put into MC passes through its walls in CC, where it is absorbed by the air-conditioner. A series of thermopiles detect the temperature of the surfaces of the measurement system and of the specimen. Determining the amount of energy transmitted by the various parts of MC and by the specimen, it is possible to apply Fourier's law to calculate the thermal conductivity of the specimen.

Keywords: straw-bale; thermal conductivity; sustainability; building

1. Introduction

Straw packaged in rectangular straw-bales (RSB), coming directly from harvesting in the field, is increasingly being used in buildings as an element of non-load-bearing walls in frame structures made of wood and steel and as a constituent element of bearing walls. The latter use has taken a decisive step with the publication of the Standard ICC IRC 2015 [1]: in Appendix S—Straw-bale Construction, a standard for the structural use of straw-bales.

In Europe, the possibility to use elements as components of buildings is affected by the actual knowledge of their physical characteristics, in particular values of their mechanical, thermal, acoustic, and fire resistance performances.

Currently, many studies have been performed on the use of natural building materials, since these materials have characteristics of high sustainability [2–9]. In particular, for straw, useful suggestions have been taken by the following studies [10–13].

From an economic point of view, only a small part of harvested straw finds profitable uses, such as bedding for livestock farms. In many situations, straw has a cost of disposal, both when it is buried and when it is burnt.

In addition, one of the major advantages of the use of the straw in construction is the possibility to supply the material locally.

In order to not lose these benefits, straw should be used in construction after harvesting without treatments, but in this way the RSB can be very different from each other. The different features

of the straw depend mainly on the growing area, the climatic conditions of the cultivation season, the procedures of harvesting and collecting, and the species and variety of cereal.

Therefore, in order to know the characteristic values [14], it is necessary to determine these values from time to time using equipment and methods relatively simple and cheap, easy to reproduce close to the area of utilization.

This research aimed to develop procedures to determine the thermal performance of RSB in the context of Tuscany Region.

To reach this goal, Standards ASTM C1363-11 [15] and UNI EN ISO 8990:1999 [16] ("Standards"), were taken as reference.

The instructions of the Standards were adopted as guidelines, but they were not completely applied. In this study, an out-and-out Hot Box was not used, but rather a low-cost system able to characterize with engineering precision the single RSB. However, the main principles and procedures of the reference Standards were followed. Also the terminology of the Standards was adopted, even if not perfectly matching to the realized system.

2. Materials and Methods

2.1. Standard and Scientific Sources

For the construction and execution of the thermal test system, the following Standards were used: ASTM C1363-11 [15]; UNI EN ISO 8990:1999 [16]; ASTM D 4442-92 (Reapproved 2003) [17]; ASTM D 4933-99 [18].

Given the peculiarities of the specimens to be tested, the information provided by these Standards were adapted to the actually existing situation.

In addition to the above-mentioned Standards, for the construction and use of the hot box, useful suggestions were taken in the following studies [19–21]. Furthermore, other suggestions were taken in studies on the thermal characterization of the materials carried out in a simplified manner [22–24].

2.2. Equipment for the Meausurement System

The design and construction of the test system and trials were carried out in laboratories of the Department of Agricultural, Food and Forestry Systems (GESAAF).

The measurement system is composed by these sub-systems: Metering Chamber (MC); Climate Chamber (CC); heaters; MC internal ventilation; CC air conditioning system; temperature measurement; air speed measurement; energy flow measurement.

The MC has the external dimensions of 1200 × 1300 × 1800 mm^3 (Figures 1 and 2).

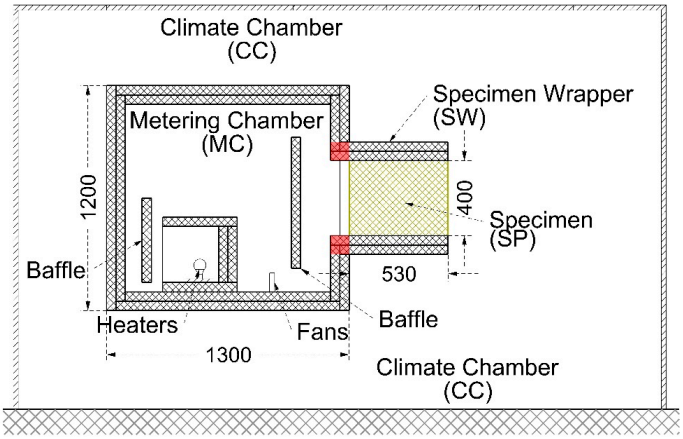

Figure 1. Sketch of a vertical section of the system.

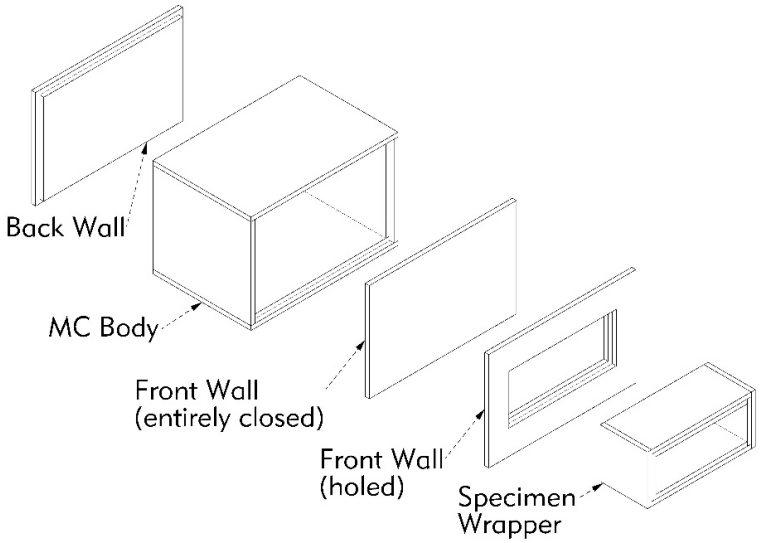

Figure 2. Exploded view of the MC.

The MC (Figures 3 and 4) is constituted by a central body, having the external dimensions of 1200 × 1200 × 1800 mm^3. The connections between the walls of the body have a labyrinthine shape, in order to reduce the loss of heat due to discontinuities.

The body can be closed by a movable flat rear wall and by a movable front wall. The front wall can be entirely closed, or provided with a hole for the positioning of the specimen. Even the connections of the body with movable walls have a labyrinthine shape.

The Specimen Wrapper (SW), designed to contain the specimen, leans out of the hole of the front wall. Inside MC a baffle is placed, to direct the flow of air generated by the fans and to prevent the inner surface of the specimen being directly exposed to the heat sources.

The walls of the MC and the SW are constituted by panels of Stiferite BB, having a nominal thickness of 50 mm. The panels are coupled, such as to form a wall of nominal thickness of 100 mm, by means of vinyl adhesive. Two layers of panel joints are staggered to minimize the possibility of heat loss through them. The typical emissivity of the bituminous paper surface is $\varepsilon = 0.93$, higher than the minimum required by [15] ($\varepsilon > 0.80$).

Stiferite BB is a sandwich panel made of an insulating component in polyisocyanurate foam, coated on both sides with bituminous paper. The mass per unit area of the 50 mm thick panel is 2.20 kg/m^2, corresponding to a density of 44.38 kg/m^3. The thermal conductivity declared by the manufacturer is $\lambda = 0.028\ Wm^{-1} \cdot k^{-1}$ (at the mean temperature of 10 °C, for 20–70 mm thickness). Since the thermal insulation properties of the foam materials decay over time and the date of manufacture was not indicated, the above value of λ is considered indicative.

Figure 3. The MC inner back view.

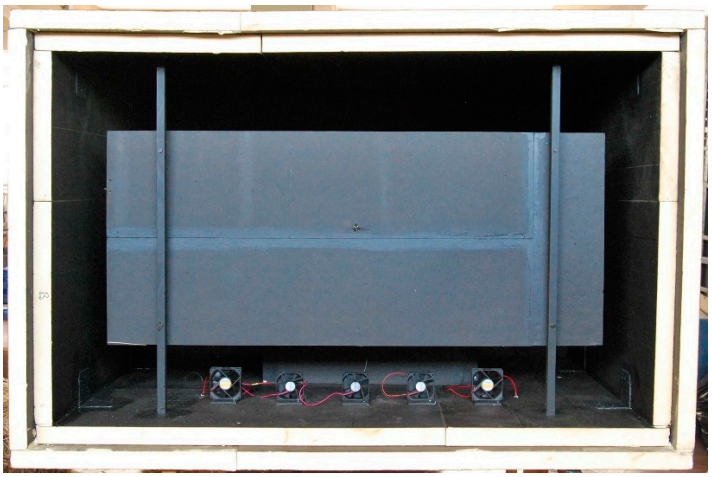

Figure 4. The MC inner front view.

The Climate Chamber (CC) is a closed space, in which the MC is placed (Figure 1).

The heat is generated by a system placed inside the MC, consisting of incandescent lamps of different power. The group is enclosed in a box of Stiferite BB closed on five sides. The open side faces a baffle of the same material to reduce the heating of the walls of the MC by direct radiation (Figure 1). The lamps can be operated individually by external control.

The internal ventilation of MC is supplied by a ventilation system composed by five computer fans, two having the rated power of 2.00 W, three having the rated power of 2.28 W.

An air conditioning system is placed inside the CC.

The surface temperature measurement system is 14 thermopiles arranged on the surfaces of the internal and external walls of the MC, of the SW, and of the specimen. One thermopile is arranged around the MC, for the measurement of the temperature of the interior of the CC. Each thermopile consists of several type K thermocouples.

The thermopiles are connected to a Pico TC08 data logger.

The measurement of the air speed is performed by means of a hot-wire probe lataOHM AP471 S2 connected to the data logger lataOHM DO9847.

The energy flow relative to heat generators and fans placed inside the MC is measured by means of a power meter (Wattmeter) PCE instruments type PCE-PA6000.

2.3. RSB Geometry and Density

The RSB is a geometrically irregular item. Its size and density can vary not only as a function of the species and varieties of cereals and of the methods of cultivation and harvesting, but also from element to element of the same origin.

To allow the actual comparison of the results of thermal tests, a measurement system of the geometry of the bales was designed. In this way, only conventional values of the dimensions and of densities were determined. However, these values are effectively comparable with each other.

For the measurement of the plant dimensions, four pinwheel walls were made, in order to follow the trend of the four vertical faces of the bales (Figure 5a).

For the measurement of plant dimensions, a horizontal force of 200 N to each pair of opposite walls has been applied.

For the measurement of the height of the edges, a straight edge having a mass of 24.30 kg was made (Figure 5b).

To determine the specimen straw moisture, the Standards [17,18] were applied. A convection oven type Orlando Valentini PRG/M 250 and a scale Kern 470 having resolution d = 0.01 g was used.

(**a**) (**b**)

Figure 5. (**a**) The four pinwheel walls for measuring the RSB plant dimensions; (**b**) The straight edge for the measurement of the straw-bale four vertical edge heights.

2.4. Preparation of the Specimen

Since the RSB have an irregular geometric shape and do not have all the same size, when the bale is placed inside the SW, it does not completely fill the internal volume. For the trials, the empty space was filled with loose straw coming from a bale of the same batch of the one to be tested. An appropriate quantity of straw was inserted in the empty spaces, such that the whole mass of straw inside the SW has the same density of the tested bale (Tables 5 and 9).

2.5. Theoretical Observations Regarding the Process

The theoretical observations regarding the process are taken by different authors [25–27].

2.5.1. Basic Observation

When energy Q_{aux} is within the MC, its internal temperature becomes higher than the temperature of the CC. This latter temperature is kept constant by an air conditioning system. Continuing to input the same energy flow Q_{aux}, when both temperatures of the MC and CC remain constant, the status of steady state has been reached. In these conditions, all the energy flow Q_{aux} entered in the interior of the MC is transmitted, through its walls, to the CC, and it is absorbed by the air conditioning system of the CC or dispersed into the surrounding environment if its temperature is lower than the CC temperature.

2.5.2. Thermal Conductivity of the Walls of the MC

Six walls of the same material and thickness L_{mc} constitute the MC.

The effective area of the MC wall normal to heat flow $A_{mc,e,eff}$ is given by [15]:

$$A_{mc,e,eff} = A_{mc,e,in} + 0.54 \cdot L_{mc} \cdot \Sigma e_i + 0.60 \cdot L_{mc}^2 \quad (1)$$

where $A_{mc,e,in}$ is the MC inside surface area, Σe_i is the sum of 12 MC interior edge lengths formed where two walls meet each other.

The quantity of energy flow introduced in MC, Q_{aux} is given by [15]:

$$Q_{aux} = Q_h + Q_f \quad (2)$$

where Q_h is the energy flow introduced by heaters, Q_f is the energy flow introduced by fans.

Applying Fourier's law, the thermal conductivity $\lambda_{mc,eff}$ of the material of the walls of the MC, in the specific temperature range, can be determined:

$$\lambda_{mc,eff} = \frac{Q_{aux} \cdot L_{mc}}{A_{mc,e,eff} \cdot (t_{mc,in} - t_{mc,out})} \quad (3)$$

where $t_{mc,in}$ is mean temperature of the internal surfaces of the walls of the MC, $t_{mc,out}$ is mean temperature of the external surfaces of the walls of the MC.

2.5.3. Thermal Conductivity of the Specimen

In the front wall of the MC there is an opening, from which a rectangular tube protrudes, named Specimen Wrapper (SW), suitable to contain the RSB to be tested. The four walls of the tube are made of the same material of the walls of the MC mentioned above.

The energy flow running through the specimen Q_{sp} is given by [15]:

$$Q_{sp} = Q_{aux} - Q_{mc,o} - Q_{fl} \quad (4)$$

where $Q_{mc,o}$ is the energy flowing through the walls of the MC, Q_{fl} is the energy flowing through the walls of the SW.

In order to determine the energy flowing through the walls of the MC ($Q_{mc,o}$), it is necessary to know the effective net area of the MC wall ($A_{mc,o,eff}$) normal to heat flow, which is given by:

$$A_{mc,o,eff} = A_{mc,e,eff} - A_{mc,o} \quad (5)$$

where $A_{mc,o}$ is the area of the opening, plus the surface, facing towards the interior of the MC of the zone highlighted in red in Figure 1.

Applying Fourier's law and knowing the thermal conductivity $\lambda_{mc,eff}$ of the material of the MC walls, in the specific temperature range, it is possible to determine the energy $Q_{mc,o}$ flowing through the walls of the MC:

$$Q_{mc,o} = \frac{\lambda_{mc,eff} \cdot A_{mc,o,eff} \cdot (t_{mc,o,in} - t_{mc,o,out})}{L_{mc}} \quad (6)$$

where $t_{mc,o,in}$ is the mean temperature of the internal surfaces of the walls of the MC, $t_{mc,o,out}$ is the mean temperature of the external surfaces of the walls of the MC.

In order to determine the energy flowing through the walls of the SW (Q_{fl}), it is important to know the effective net area of the SW wall ($A_{fl,eff}$), normal to heat flow. It is given by the relation [15]:

$$A_{fl,eff} = A_{flin} + 0.54 \cdot L_{mc} \cdot \Sigma e_i + 0.60 \cdot L_{mc}^2 \quad (7)$$

where $A_{fl,in}$ is the internal area of the SW, minus the surface, facing towards the interior of the SW, of the zone highlighted in Figure 1; Σe_i is the sum of 4 SW interior edge lengths formed where two walls meet each other, minus the lengths of the edges in correspondence of the zone highlighted in red in Figure 1.

Applying the Fourier law and knowing the thermal conductivity $\lambda_{mc,eff}$ of the material of the SW, in the specific temperature range, previously determined, it is possible to determine the energy flow (Q_{fl}) flowing through the walls of the SW:

$$Q_{fl} = \frac{\lambda_{mc,eff} \cdot A_{fl,eff} \cdot (t_{fl,in} - t_{fl,out})}{L_{mc}} \quad (8)$$

where $t_{fl,in}$ is the mean temperature of the internal surfaces of the walls of the SW and $t_{fl,out}$ is the mean temperature of the external surfaces of the walls of the SW.

Applying (4), the value of the energy flow passing through the specimen, Q_{sp}, can be obtained.

Applying the Fourier law, the value of the thermal conductivity λ_{sp} of the specimen relative to the actual test conditions can be obtained:

$$\lambda_{sp} = \frac{Q_{sp} \cdot L_{sp}}{A_{mc,o} \cdot (t_{sp,1} - t_{sp,2})} \quad (9)$$

where L_{sp} is the length of the specimen in the prevailing direction of the energy flow, $t_{sp,1}$ is the mean temperature of the hot surface of the specimen, and $t_{sp,2}$ is the mean temperature of the cold surface of the specimen.

2.6. Main Simplifications

In addition to those suggested by the [15], the most significant simplifications introduced are the following:

a. Fourier's law

The Fourier's law in its one-dimensional (x) form is used (see Table 1):

$$q_x = \frac{dJ_x}{dT} = \lambda \cdot \frac{dt}{dx} \quad (10)$$

For two points at constant temperature, at a distance Δx (see Table 1):

$$Q = \lambda \cdot \frac{A \cdot \Delta t}{\Delta x} \quad (11)$$

Table 1. Symbology.

Energy, Heat	J	$(kg \cdot m^2 \cdot s^{-2})$
Time	T	s
Temperature	t	°C, K
Heat Flow density, time rate of heat flow through a unit area	q	$W \cdot m^{-2}$
Heat Flow, time rate of net heat flow through the area A	Q	W $(J \cdot s^{-1})$
Apparent thermal conductivity	λ	$Wm^{-1} \cdot K^{-1}$

b. Geometry and density of straw-bales and of the specimen

For this purpose, the system described in Section 2.3 was designed and operated.

c. Energy flows

The energy flow that occurs between the MC and CC through the area marked in red in Figure 1 is very complex. In this zone, the heat exchange between the MC and CC is not direct, but occurs through the adjacent zones of the walls of MC. The definition of the way in which this heat exchange occurs requires a dedicated study, which will be performed in a second step of the research. In this work, considering that the surface of the zone in question is relatively small compared to the total, the effects of this singularity are neglected.

d. Air flows

The specimen shall be sealed relating to exchanges of air with the MC and the CC. For this purpose, two surfaces in contact with MC and with CC were closed by means of a film of Linear Low-Density Polyethylene (LLDPE), having a thickness of 23 μm and thermal conductivity of 0.33 $Wm^{-1} \cdot K^{-1}$.

The connections of the detachable walls with adhesive tape were sealed.

e. Effective areas

The Equations (1) and (7) are derived by applying to this particular case the relation (A3.2) of the ASTM [15], which is given for a chamber having five walls, that is eight edges. In this case, there are respectively 12 and 4 edges: relations are calculated using the corresponding values of the two cases.

3. Results and Discussion

3.1. Thermal Conductivity of the Walls of the MC

To implement this test, the MC was entirely closed. The MC walls were all identical in terms of material and thickness. Thermopiles and thermocouples were arranged as shown in Table 2.

Table 2. Thermopiles and thermocouples arrangement.

Equipment		Thermopiles		Thermocouples	
		Internal	**External**	**Internal**	**External**
MC	Left	1	2	4	4
	Right	1	2	4	4
	Top	3	4	6	6
	Bottom	5	6	5	5
	Front	7	8	6	6
	Back	9	10	6	6
CC		17			6

Considering that the diffusion of heat on the left and right walls is symmetrical, there was only one thermopile for their internal surfaces and one for the external ones.

The test was carried out from 16 March 2015 11:47 to 22 March 2015 13:27. For the calculation, the data related to the time interval 21 March 2015 12:27 to 21 March 2015 23:17 were used. The data were collected with an interval of 10 min. The results are summarized in Table 3.

Table 3. Determination of the Thermal Conductivity of the walls of the MC.

Climate Chamber Temperature	$\mathbf{t_{cc}}$	**5.05**	**°C**
Air speed, near the hot side of the specimen	as_{sp}	0.31	m/s
Metering Chamber inside surface area	$A_{mc,in}$	8.92	m^2
Metering Chamber wall thickness	L_{mc}	0.103	m
Sum of all (total of 12) Metering Chamber interior edge lengths formed where two walls meet	Σe_i	14.80	m
Metering Chamber effective area normal to heat flow	$A_{mc,eff}$	9.75	m^2
Metering Chamber inside wall surface temperature	$t_{mc,in}$	31.22	°C
Metering Chamber outside wall surface temperature	$t_{mc,out}$	7.32	°C
Net heat added by the heaters	Q_h	56.61	W
Net heat added by the fans	Q_f	10.31	W
Net heat removed by the cooling coil	Q_c	0.00	W
Net heat flow due to the fan, heater, and cooling coil	Q_{aux}	66.92	W
Metering Chamber wall thermal conductivity	$\lambda_{mc,eff}$	0.030	$W \cdot m^{-1} \cdot K^{-1}$

3.2. Thermal Conductivity of the Specimen SB01

To implement this test, the MC was closed with the holed front wall bearing the SW. The MC and SW walls are all identical, in terms of material and thickness. Thermopiles and thermocouples were arranged as shown in Table 4.

Table 4. Thermopiles and thermocouples arrangement.

Equipment		Thermopiles		Thermocouples	
		Internal	**External**	**Internal**	**External**
MC	Left	1	2	4	4
	Right	1	2	4	4
	Top	3	4	6	6
	Bottom	5	6	5	5
	Front	7	8	6	6
	Back	9	10	6	6
SW	Path 1	11	12	8	8
	Path 2	13	14	8	8
Specimen	Hot side	15		9	
	Cold side		16		9
CC			17		6

Considering that the diffusion of heat on the left and right walls of MC is symmetrical, there was only one thermopile for their internal surfaces and one for the external ones. The geometrical dimensions and density of the RSB were conventionally determined as illustrated in Section 2.3 (Figure 6).

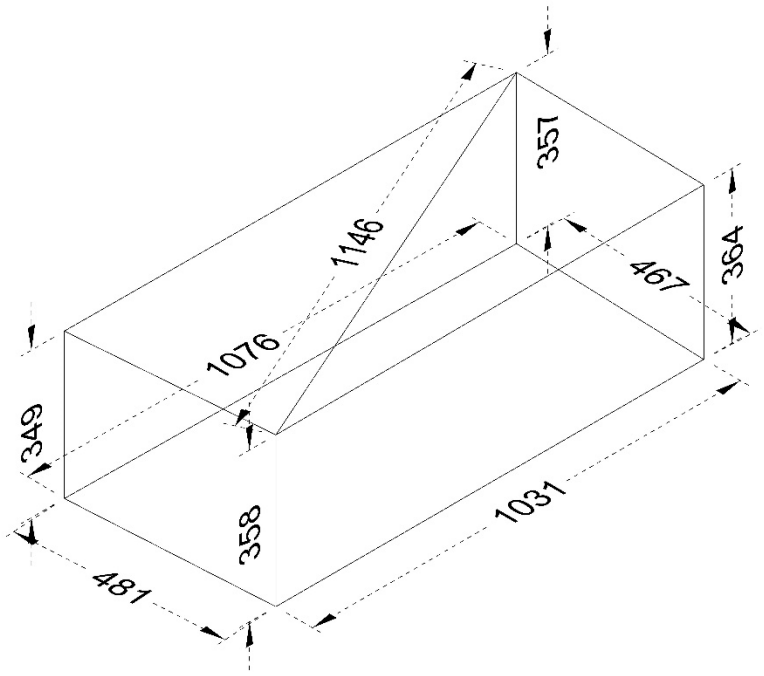

Figure 6. SB01 dimensions.

The specimen was prepared as described in Section 2.4. (See also Table 5).

Table 5. Dimensions and density of the RSB and of the specimen.

RSB (Code)	RSB Volume (m^3)	RSB Mass (kg)	RSB Density (kg/m^3)	Cereal Species	Cereal Origin	SW Internal Volume (m^3)	Specimen Mass (kg)	Mass Added to Fill SW (kg)
SB01	0.178	11.70	65.69	*Triticosecale*	Sorano (GR)	0.237	15.60	3.90

The moisture of the specimen was determined as described in Section 2.3 and results are shown in Table 6.

Table 6. Specimen straw moisture.

RSB (Code)	Sample (ID)	Unladen Mass (g)	Starting Straw Mass (g)	Starting Mass (g)	Controll Mass (g)	Final Straw Mass (g)	Water Content (g)	Moisture Content (%)
SB01	M01	96.39	58.07	154.46	148.01	51.62	6.45	12.50
	M02	91.43	50.18	141.61	136.18	44.75	5.43	12.13
	M03	95.11	63.10	158.21	151.34	56.23	6.87	12.22
	M04	90.37	67.97	158.34	150.77	60.40	7.57	12.53

The test was carried out from 23 March 2015 16:38 to 27 March 2015 10:18. For the calculation the data related to the time interval 26 March 2015 16:08 to 26 March 2015 21:38 were used. The data were collected with a time interval of 10 min. The test results are summarized in Table 7.

Table 7. Calculation of the thermal conductivity of the specimen SB01.

Climate Chamber Temperature	t_{cc}	**5.830**	°C
Air speed, near the hot side of the specimen	as_{sp}	0.315	$m \cdot s^{-1}$
Metering Chamber inside surface area	$A_{mc,in}$	8.920	m^2
Metering Chamber wall thickness	L_{mc}	0.103	m
Sum of 12 Metering Chamber interior edge lengths formed where two walls meet	Σ_{ei}	14.800	m
Metering Chamber effective area normal to heat flow	$A_{mc,eff}$	9.750	m^2
Metering Chamber inside wall surface temperature	$t_{mc,in}$	31.83	°C
Metering Chamber outside wall surface temperature	$t_{mc,out}$	8.277	°C
Net heat added by the heaters	Q_h	58.26	W
Net heat added by the fans	Q_f	10.604	W
Net heat removed by the cooling coil	Q_c	0.00	W
Net heat flow due to the fan, heater, and cooling coil	Q_{aux}	67.430	W
Metering Chamber wall thermal conductivity	$\lambda_{mc,eff}$	0.030	$W \cdot m^{-1} \cdot K^{-1}$
Metering Chamber opening area	$A_{mc,o}$	0.792	m^2
Metering Chamber net area	$A_{mc,eff,n}$	8.958	m^2
Metering Chamber wall loss	Q_{mc}	61.452	W
Specimen Wrapper inside surface area	$A_{sw,in}$	1.307	m^2
Specimen Wrapper wall thickness	L_{sw}	0.103	m
Sum of all (total of 4) Specimen Wrapper interior edge lengths formed where two walls meet	$\Sigma e_{sw,i}$	1.720	m
Specimen Wrapper effective area perpendicular to the heat flow passing through it	$A_{sw,eff}$	1.409	m^2
Length of the heat flow path (test specimen)	L_{sp}	0.530	m
Specimen Wrapper wall thermal conductivity	$\lambda_{sw,eff}$	0.030	$W \cdot m^{-1} \cdot K^{-1}$
Specimen Wrapper inside wall surface temperature	$t_{sw,in}$	16.457	°C
Specimen Wrapper outside wall surface temperature	$t_{sw,out}$	7.457	°C
Specimen Wrapper wall heat loss	Q_{sw}	3.694	W
Specimen heat flow	Q_{sp}	2.283	W
Specimen hot surface temperature	$t_{sp,1}$	31.388	°C
Specimen cold surface temperature	$t_{sp,2}$	6.698	°C
Apparent thermal conductivity of the specimen	λ_{sp}	0.062	$W \cdot m^{-1} \cdot K^{-1}$

3.3. Thermal Conductivity of the Specimen SB02

To implement this test, the thermopiles and thermocouples were arranged as shown in Table 4.

Considering that the diffusion of heat on the left and right walls of MC is symmetrical, there was only one thermopile for their internal surfaces and one for the external ones.

The geometrical dimensions and density of the RSB were conventionally determined as illustrated in Figure 7.

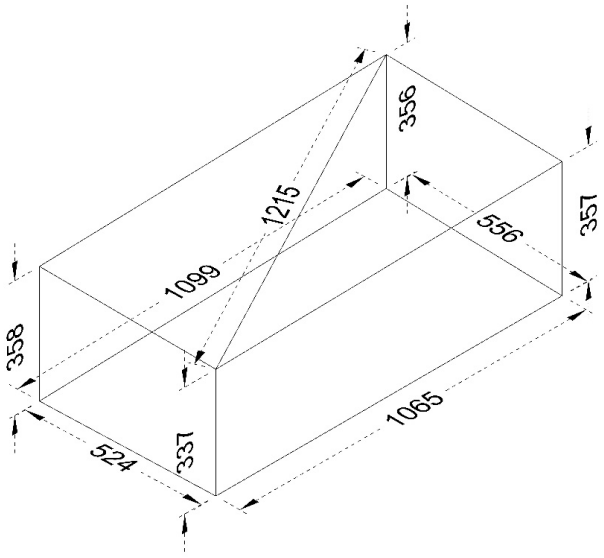

Figure 7. SB02 dimensions.

The specimen was prepared as described in Section 2.4 (see also Table 8).

Table 8. Dimensions and density of the straw-bale and of the specimen SB02.

RSB (Code)	RSB Volume (m^3)	RSB Mass (kg)	RSB Density (kg/m^3)	Cereal Species	Cereal Origin	SW Internal Volume (m^3)	Specimen Mass (kg)	Mass Added to Fill SW (kg)
SB02	0.205	17.20	84.11	*Triticum turgidum durum*	Vicarello (PI)	0.237	19.97	2.77

The moisture of the specimen was determined as described in Section 2.3 and results are shown in Table 9.

Table 9. Specimen straw moisture.

RSB (Code)	Sample (ID)	Unladen Mass (g)	Starting Straw Mass (g)	Starting Mass (g)	Controll Mass (g)	Final Straw Mass (g)	Water Content (g)	Moisture Content (%)
SB02	M01	96.39	86.59	182.98	174.33	77.79	8.80	11.31
	M02	91.43	77.10	168.53	160.60	68.99	8.11	11.76
	M03	95.11	41.20	136.31	132.10	36.99	4.21	11.38
	M04	90.37	54.73	145.10	139.11	48.94	5.79	11.83

The test was carried out from 8 April 2015 10:30 to 10 April 2015 11:10. For the calculation the data related to the time interval 9 April 2015 21:10 to 10 April 2015 08:10 were used. The data were collected with a time interval of 10 min. The test results are summarized in Table 10.

Table 10. Calculation of the thermal conductivity of the specimen SB02.

Climate Chamber Temperature	t_{cc}	5.815	°C
Air speed, near the hot side of the specimen	as_{sp}	0.315	$m \cdot s^{-1}$
Metering Chamber inside surface area	$A_{mc,in}$	8.920	m^2
Metering Chamber wall thickness	L_{mc}	0.103	m
Sum of all (total of 12) Metering Chamber interior edge lengths formed where two walls meet	Σe_i	14.800	m
Metering Chamber effective area normal to heat flow	$A_{mc,eff}$	9.750	m^2
Metering Chamber inside wall surface temperature	$t_{mc,in}$	31.727	°C
Metering Chamber outside wall surface temperature	$t_{mc,out}$	8.272	°C
Net heat added by the heaters	Q_h	56.826	W
Net heat added by the fans	Q_f	10.604	W
Net heat removed by the cooling coil	Q_c	0.000	W
Net heat flow due to the fan, heater, and cooling coil	Q_{aux}	67.430	W
Metering Chamber wall thermal conductivity	$\lambda_{mc,eff}$	0.030	$W \cdot m^{-1} \cdot K^{-1}$
Metering Chamber opening area	$A_{mc,o}$	0.792	m^2
Metering Chamber net area	$A_{mc,eff,n}$	8.958	m^2
Metering Chamber wall loss	Q_{mc}	61.194	W
Specimen Wrapper inside surface area	$A_{sw,in}$	1.307	m^2
Specimen Wrapper wall thickness	L_{sw}	0.103	m
Sum of all (total of 4) Specimen Wrapper interior edge lengths formed where two walls meet	$\Sigma e_{sw,i}$	1.720	m
Specimen Wrapper effective area perpendicular to the heat flow passing through it	$A_{sw,eff}$	1.409	m^2
Length of the heat flow path (test specimen)	L_{sp}	0.530	m
Specimen Wrapper wall thermal conductivity	$\lambda_{sw,eff}$	0.030	$W \cdot m^{-1} \cdot K^{-1}$
Specimen Wrapper inside wall surface temperature	$t_{sw,in}$	16.159	°C
Specimen Wrapper outside wall surface temperature	$t_{sw,out}$	7.106	°C
Specimen Wrapper wall heat loss	Q_{sw}	3.716	W
Specimen heat flow	Q_{sp}	2.520	W
Specimen hot surface temperature	$t_{sp,1}$	31.040	°C
Specimen cold surface temperature	$t_{sp,2}$	6.994	°C
Apparent Thermal Conductivity of the Specimen	λ_{sp}	0.070	$W \cdot m^{-1} \cdot K^{-1}$

The value of the thermal conductivity of the walls of the MC (λ = 0.030 $Wm^{-1} \cdot k^{-1}$) is congruent with the value of the thermal conductivity declared by the manufacturer (λ = 0.028 $Wm^{-1} \cdot k^{-1}$) of the base material for the reason mentioned in the Section 2.2.

The values of the thermal conductivity of the specimens (SB01 and SB02) experimentally determined are consistent with values found in the scientific literature [28,29]. Therefore, it is reasonable to consider that the system leads to results of sufficient accuracy for the purpose of the research.

However, the results are extremely sensitive to the values instrumentally detected, in particular to the value of the energy flow fed into the MC and the values of the internal temperatures of the MC and the SW. In consequence of this criticality, the instrumental measurements of these quantities must be made with great accuracy and this involves the use of instrumentation and procedures too expensive and complicated with respect to the intentions of this research.

Moreover, it is important to remember that the influence of the area marked in red in Figure 1 was not studied in this research. For these reasons, the research must be developed, especially with the intent to reduce the influence of the criticalities above reported in significant quantities.

4. Conclusions

The aim of the research is the identification of simple and economic equipment and procedures that can be replicated in proximity to the area of use of RSB. These methods should be suitable for the determination of the values of thermal conductivity of RSB actually available on site for building, although not of absolute precision.

The ways to reach this goal may be mainly two:

(a) to modify the current system in order to reduce the sensitivity of the system to the values of energy flow and temperatures instrumentally detected;

(b) to design and implement a system that, instead of trying to determine the absolute value of the thermal conductivity of the specimens, determines the relative value compared to specimens of materials having a known value of thermal conductivity.

Currently, it can be assumed that method (b) can be realized with tools and procedures simpler and cheaper than these required by method (a). The implementation of a transportable version, from time to time, on the zones of effective use of straw-bales, can even be hypothesized.

Future developments will be aimed to continue tests in this direction, with the purpose to reduce the uncertainty margins of results, mainly due to some of the adopted simplifications.

Acknowledgments: The authors gratefully acknowledge Ente Cassa di Risparmio di Firenze for the financial support of the project.

Author Contributions: Leonardo Conti conceived and designed the research. Leonardo Conti collected and processed the data. Leonardo Conti, Matteo Barbari, and Massimo Monti wrote the manuscript until its final version.

Conflicts of Interest: The authors declare no conflict of interest.

References

1. International Code Council (ICC). *International Residential Code for One-End Two-Family Dwellings*; International Code Council: Washington, DC, USA, 2015; pp. 776–789. Available online: http://codes.iccsafe.org/app/book/content/2015-I-Codes/2015%20IRC%20HTML/Appendix%20S.html (accessed on 20 December 2014).
2. Asdrubali, F.; D'Alessandro, F.; Schiavoni, S. A review of unconventional sustainable building insulation materials. *Sust. Mater. Technol.* **2015**, *4*, 1–17. [CrossRef]
3. Korjenic, A.; Petránek, V.; Zachb, J.; Hroudová, J. Development and performance evaluation of natural thermal-insulation materials composed of renewable resources. *Energy Build.* **2011**, *43*, 2518–2523. [CrossRef]
4. Luamkanchanaphan, T.; Chotikaprakhan, S.; Jarusombati, S. A Study of Physical, Mechanical and Thermal Properties for Thermal Insulation from Narrow-leaved Cattail Fibers. *APCBEE Procedia* **2012**, *1*, 46–52. [CrossRef]
5. Muizniece, I.; Lauka, D.; Blumberga, D. Thermal Conductivity of Freely Patterned Pine and Spruce Needles. *Energy Procedia* **2015**, *72*, 256–262. [CrossRef]
6. Paiva, A.; Pereiraa, S.; Sá, A.; Cruz, D.; Varum, H.; Pinto, J. A contribution to the thermal insulation performance characterization of corn cob particleboards. *Energy Build.* **2012**, *45*, 274–279. [CrossRef]
7. Zacha, J.; Korjenic, A.; Petráneka, V.; Hroudová, J.; Bednar, T. Performance evaluation and research of alternative thermal insulations based on sheep wool. *Energy Build.* **2012**, *49*, 246–253. [CrossRef]

8. Belhadj, B.; Bederina, M.; Makhloufia, Z.; Goullieux, A.; Quéneudec, M. Study of the thermal performances of an exterior wall of barley straw sand concrete in an arid environment. *Energy Build.* **2015**, *87*, 166–175. [CrossRef]
9. Conti, L.; Barbari, M.; Monti, M. Design of Sustainable Agricultural Buildings. A Case Study of a Wine Cellar in Tuscany, Italy. *Buildings* **2016**, *6*. [CrossRef]
10. Pruteanu, M. Investigations Regarding the Thermal Conductivity of Straw. *Bul. Inst. Politeh. Din Iaşi* **2010**, *56*, 9–16.
11. Wei, K.; Lv, C.; Chen, M.; Zhou, X.; Dai, Z.; Shen, D. Development and performance evaluation of a new thermal insulation material from rice straw using high frequency hot-pressing. *Energy Build.* **2015**, *87*, 116–122. [CrossRef]
12. Ashour, T.; Georg, H.; Wu, W. Performance of straw-bale wall: A case of study. *Energy Build.* **2011**, *43*, 1960–1967. [CrossRef]
13. Shea, A.D.; Wall, K.; Walker, P. Evaluation of the thermal performance of an innovative prefabricated natural plant fibre building system. *Build. Serv. Eng. Res. Technol.* **2013**, *34*, 369–380. [CrossRef]
14. *UNI 10351 Materiali da Costruzione. Conduttività Termica e Permeabilità al Vapore*; UNI: Milano, Italia, 1994; pp. 1–16.
15. *ASTM C1363-11 Standard Test Method for Thermal Performance of Building Materials and Envelope Assemblies by Means of a Hot Box Apparatus*; ASTM: West Conshohocken, PA, USA; pp. 1–44. Available online: http://www.astm.org/Standards/C1363.htm (accessed on 20 January 2015).
16. *UNI EN ISO 8990:1994 Thermal Insulation—Determination of Steady-State Thermal Transmission Properties—Calibrated and Guarded Hot Box*; UNI: Milano, Italia, 1999; pp. 1–28. Available online: http://www.iso.org/iso/catalogue_detail.htm?csnumber=16519 (accessed on 27 January 2015).
17. *ASTM D 4442-92 (Reapproved 2003) Standard Test Methods for Direct Moisture Content Measurement of Wood and Wood-Base Materials*; ASTM: West Conshohocken, PA, USA, 2003; pp. 1–6. Available online: http://www.astm.org/DATABASE.CART/HISTORICAL/D4442-92R03.htm (accessed on 27 January 2015).
18. *ASTM D 4933-99 Standard Guide for Moisture Conditioning of Wood and Wood-Based Materials*; ASTM: West Conshohocken, PA, USA, 1999; pp. 1–8. Available online: https://www.astm.org/Standards/D4933.htm (accessed on 21 January 2015).
19. Ghosha, A.; Ghosh, S.; Neogia, S. Performance Evaluation of a Guarded Hot Box U-value Measurement Facility under Different Software based Temperature Control Strategies. *Energy Procedia* **2014**, *54*, 448–454. [CrossRef]
20. Kus, H.; Özkan, E.; Göcer, Ö.; Edis, E. Hot box measurements of pumice aggregate concrete hollow block walls. *Constr. Build. Mater.* **2013**, *38*, 837–845. [CrossRef]
21. Miller, R.G. Hot Box Operating Techniques and Procedures: A Survey. *J. Test. Eval.* **1987**, *15*, 153–166.
22. Derbal, R.; Defer, D.; Chauchois, A.; Antczak, E. A simple method for building materials thermophysical properties estimation. *Constr. Build. Mater.* **2014**, *63*, 197–205. [CrossRef]
23. Ladevie, B.; Fudym, O.; Batsale, J.C. A new simple device to estimate thermophysical properties of insulating materials. *Int. Commun. Heat Mass Transf.* **2000**, *27*, 473–484. [CrossRef]
24. Yesilata, B.; Turgut, P. A simple dynamic measurement technique for comparing thermal insulation performances of anisotropic building materials. *Energy Build.* **2007**, *39*, 1027–1034. [CrossRef]
25. Fermi, E. *Termodinamica*; Bollati Boringhieri: Torino, Italia, 1958.
26. Poggi, L. *Termotecnica*, 2nd ed.; Vallerini: Pisa, Italia, 1971.
27. Sears, F.W. *Mechanics, Heat and Sound*, 2nd ed.; Addison-Wesley Publishing Company, Inc.: Boston, MA, USA, 1958.
28. Ashour, T.; Wieland, H.; Georg, H.; Bockisch, F.J.; Wu, W. The influence of natural reinforcement fibres on insulation values of earth plaster for straw bale buildings. *Mater. Des.* **2010**, *31*, 4676–4685. [CrossRef]
29. Goodhew, S.; Griffiths, R. Sustainable earth walls to meet the building regulations. *Energy Build.* **2005**, *37*, 451–459. [CrossRef]

© 2016 by the authors; licensee MDPI, Basel, Switzerland. This article is an open access article distributed under the terms and conditions of the Creative Commons Attribution (CC-BY) license (http://creativecommons.org/licenses/by/4.0/).